ELSEVIER

Journal of Materials Processing Technology 83 (1998) 151–158

Journal of Materials Processing Technology

Machining of Al/SiC particulate metal-matrix composites Part I: Tool performance

M. El-Gallab [a], M. Sklad [b,*]

[a] Pratt and Whitney Canada, Mississauga, Ontario, L5T 1J3, Canada
[b] Department of Mechanical Engineering, McMaster University, Hamilton, Ontario, L8S 4L7, Canada

Received 20 March 1997

Abstract

Despite the superior mechanical and thermal properties of particulate metal-matrix composites, their poor machinability has been the main deterrent to their substitution for metal parts. The hard abrasive reinforcement phase causes rapid tool wear during machining and, consequently, high machining costs. A series of dry high-speed turning tests were performed to select the optimum tool material, tool geometry and cutting parameters for the turning of 20%SiC/Al metal-matrix composites. The results indicate that polycrystalline diamond tools (PCD) provide satisfactory tool life compared to alumina and coated-carbide tools, where the latter tools suffered from excessive edge chipping and crater wear during the machining of the metal-matrix composite under study. Furthermore, the cost of PCD tools could be justified by using dry cutting at feed rates as high as 0.45 mm rev^{-1}, cutting speeds of 894 m min^{-1} and a depth of cut of 1.5 mm. With these cutting parameters, the relatively small built-up edge formed on the tool protects it from further wear by abrasion and micro-cutting. Polycrystalline tools with zero rake angle and large tool nose radii are recommended for the roughing operations.

Keywords: Metal-matrix composites; Tool wear

1. Introduction

Metal-matrix composites (MMCs) form one group of the new engineered materials that have received considerable research since the trials by Toyota in the early 1980s [1]. The most popular reinforcements are silicon carbide and alumina. Aluminium, titanium and magnesium alloys are commonly used as the matrix phase. The density of most MMCs is approximately one third that of steel, resulting in high specific strength and stiffness [2]. Due to these potentially attractive properties coupled with the inability to operate at high temperatures, MMCs compete with super-alloys, ceramics, plastics and re-designed steel parts in several aerospace and automotive applications. The latter materials, however, may not have much further capacity for the inevitable future increases in service loads [3].

Particulate metal-matrix composites (PMMCs) are of particular interest, since they exhibit higher ductility and lower anisotropy than fiber reinforced MMCs [2]. Moreover, PMMCs offer superior wear resistance [3]. While many engineering components made from PMMCs are produced by the near net shape forming and casting processes, they frequently require machining to achieve the desired dimensions and surface finish. The machining of PMMCs presents a significant challenge, since a number of reinforcement materials are significantly harder than the commonly used high-speed steel (HSS) and carbide tools [4]. The reinforcement phase causes rapid abrasive tool wear and therefore the widespread usage of PMMCs is significantly impeded by their poor machinability and high machining costs.

2. Literature review

From the available literature on PMMCs, it is clear

* Corresponding author. Fax: +1 905 5727944; e-mail: mechmac@mcmaster.ca

0924-0136/98/$19.00
PII S0924-0136(98)00054-5

Table 1
Typical physical properties of Duralcan F3S.20S [20]

Property	
Density (g cm^{-3})	2.77
Thermal conductivity (cal cm^{-1} s^{-1} K^{-1}) at 22°C	0.47
Specific heat (cal g^{-1} K)	
100°C	0.218
200°C	0.239
300°C	0.259
Average coefficient of thermal expansion	
50–100°C	17.5
50–300°C	21.1
50–500°C	21.4
Ultimate strength (MPa)	262
Yield strength (MPa)	21.4
Elongation (%)	1.9
Elastic modulus (GPa)	98.6
Rockwell hardness (B)	67 ± 1.5

Table 2
Tool geometry

Tool	Geometry
PCD (tipped-80°rhomboid)	Rake angle, α: −5°, 0°, 5°
	Clearance angle: 7°
	Approach angle: 5°
	Tool nose radius (mm), r: 0.8, 1.6
TiN coated carbide (triangular)	Rake angle, α: 0°
	Clearance angle: 7°
	Approach angle: 5°
	Tool nose radius (mm), r: 1.6
Al_2O_3/TiC ceramic (triangular)	Rake angle, α: 0°
	Clearance angle: 7°
	Approach angle: 5°
	Tool nose radius (mm), r: 1.6

that the morphology, distribution and volume fraction of the reinforcement phase, as well as the matrix properties, are all factors that affect the overall cutting process [2,4], but as yet relatively few works related to the optimization of the productivity process have been pulished. For example, Monaghan [2] studied the wear mechanism of carbide tools during the machining of 25% SiC/Al PMMC at speeds below 20 m min^{-1}. Tomac et al. [5] developed a tool life relationship for carbide tools during the machining of SiC/Al PMMCs at speeds lower than 100 m min^{-1}. However, the authors of Ref. [5] recommended further research on the built-up edge phenomenon that is observed in all tools during the machining of SiC/Al PMMCs. O'Reilly et al. [6] ranked various tool materials with respect to tool wear, however, their cutting parameters did not exceed 125 m min^{-1} and 1.0 mm depth of cut, which was achieved using cubic boron nitride tools. Similar test results were reported by Brun et al. [7] who related the tool wear rate, mainly due to abrasion, to the tool hardness. Winert [8] attributed the wear of the carbide tools to abrading Al_2O_3 particles that form on the surface and rub the tool in the direction of the chip flow. However, pulled SiC particles could also lead to the same effect, SiC particles also being harder than the WC. Tomac et al. [5] suggested that coatings with less hardness than that of Al_2O_3 and SiC offer little to no advantage during the machining of SiC/Al PMMCs, Brun et al. [7] suggested using lower cutting speeds to reduce the cutting temperature, which accelerate diffusion and adhesion wear and thermally weaken the tool. Since aluminium tends to seize on the tool face and since grain boundaries are the sites of seizure, the authors recommended using cemented carbide tools with a large grain size.

Several researchers [7–25] have indicated that polycrystalline diamond (PCD) tools are the only tool material that is capable of providing a useful tool life during the machining of SiC/Al PMMCs. PCD is harder than Al_2O_3 and SiC and does not have a chemical tendency to react with the workpiece material. Tomac et al. [5] compared the performance of chemical vapor deposition (CVD) inserts to that of TiN, Ti(CN) and Al_2O_3 coated tools. CVD tools offered better overall performance than that of the other tools. Lane et al. [18] studied the performance of different CVD tools with thin and thick films. According to their observations, CVD tools with thin films failed catastrophically during the end milling of 20%SiC/Al PMMC. This tool failure was attributed to coating spalling and consequent damage to the relatively soft carbide substrate. Furthermore, PCD tools with a grain size of 25 μm better withstand abrasion wear by micro-cutting than tools with a grain size of 10 μm [8,14]. Further increases in PCD grain size do not benefit the tool life, but rather cause significant deterioration in the surface finish. This

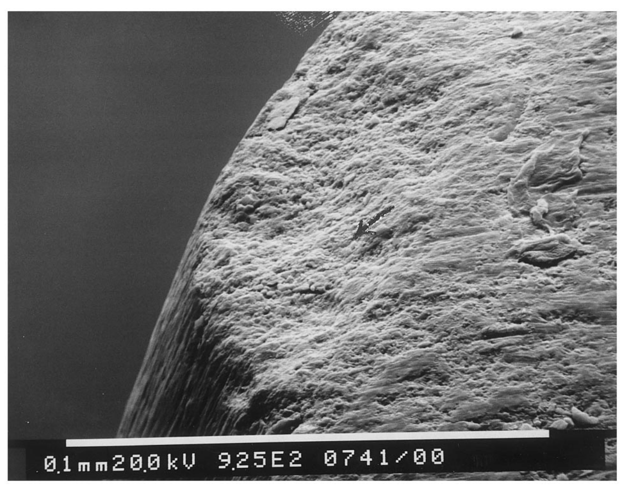

Fig. 1. SEM figure showing wear on Al_2O_3 tool ($v = 488$ m min^{-1}, $f = 0.2$ mm rev^{-1}, $doc = 0.5$ mm, $r = 1.6$ mm, $\alpha = 0°$).

Table 3
Effect of tool material on cutting forces and temperatures ($r = 1.6$ mm; $\alpha = 0°$)

Tool material	Measured cutting force (N)	Measured cutting temperature (°C)
PCD ($v = 894$ m min^{-1}; $f = 0.45$ mm rev^{-1}; $doc = 2.5$ mm)	97.00	440
PCD ($v = 670$ m min^{-1}; $f = 0.25$ mm rev^{-1}; $doc = 1.5$ mm)	98.10	410
Al_2O_3 ($v = 248$ m min^{-1}; $f = 0.2$ mm rev^{-1}; $doc = 0.5$ mm)	183.85	520
TiN ($v = 248$ m min^{-1}; $f = 0.2$ mm rev^{-1}; $doc = 0.5$ mm)	143.52	500

is because PCD grains with size > 25 μm are easily pulled out of the cutting edge.

Regarding the effect of the cutting parameters on the tool life, Lane et al. [11–15,17–19] attributed the increase in the wear of PCD tools (by abrasion) to increase in kinetic energy gained by abrading SiC particles. On the other hand, Brun et al. [7] attributed the increase in tool wear in the thermal degradation of the tool material. Tool wear was found to be inversely proportional to the feed rate [9]. Tomac et al. [5] attributed the increase in tool life at higher feed rates to the thermal softening of the composite. The authors suggest that the workpiece material becomes softer and the SiC particles become pressed into the workpiece, causing less abrasion on the tool itself. However, Finn et al. [24] and Morin et al. [25] attributed the reduction in tool wear with greater feed rates to the reduced contact between the cutting edge and the abrasive SiC particles. Despite the controversy in explaining the mechanism behind the tool wear at different feed rates, all researchers recommend using feed rates and depths of cut that are as aggressive as possible during the roughing operations. Finally, with regard to the coolant application, researchers at Duralcan USA [11–23], recommend investigating the possibility of dry-rough machining in order to take advantage of the 'protective built-up edge phenomenon.'

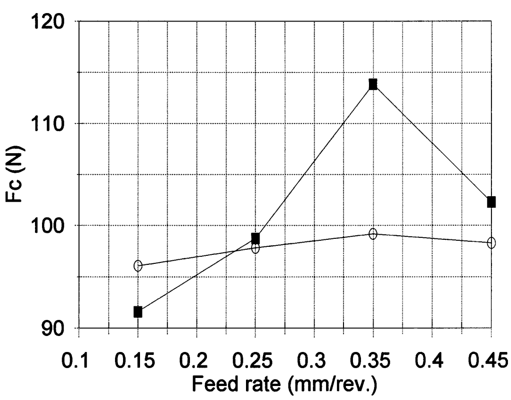

Fig. 2. Effect of cutting speed on the cutting forces (PCD tool: $r = 1.6$ mm, $\alpha = 0°$; square points: $v = 670$ m min^{-1}, $doc = 1.5$ mm; round points: $v = 894$ m min^{-1}, $doc = 1.5$ mm).

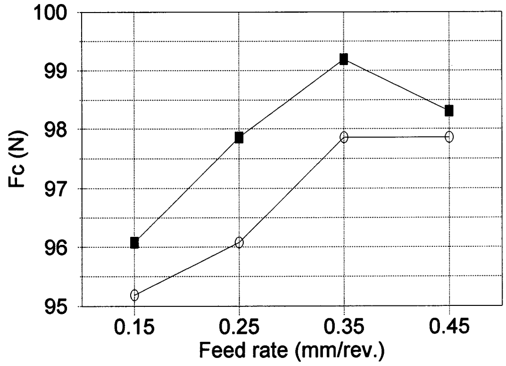

Fig. 3. Effect of depth of cut on the cutting forces (PCD tool: $r = 1.6$ mm, $\alpha = 0°$; square points: $v = 894$ m min^{-1}, $doc = 1.5$ mm; round points: $v = 894$ m min^{-1}, $doc = 2.5$ mm).

In summary, the literature review carried out showed that the effect of more aggressive cutting parameters (speed, feed and depth of cut) still needs further research in order to improve the economics of the cutting process. Also, several important parameters have been overlooked by previous researchers, among which are the tool geometry and coolant application.

3. Test material and cutting tools

3.1. Workpiece material

The machining investigations were carried out using Duralcan F3S.20S Al/SiC metal-matrix composite. The SiC particles had an average diameter of 12 μm. Table 1 shows some of the physical and mechanical properties of A356-20%SiC PMMC. Prior to carrying out the cutting experiments, the test material was fully heat-treated to the T71 condition. The test material was in the form of bars of 177.8 mm diameter and 305 mm length.

3.2. Cutting tools

Various tool materials (coated carbide, Al_2O_3/TiC and PCD) and geometries were employed in the study. Oblique turning tests were carried out and different cutting parameters were employed for each tool material. However, for the purpose of comparing tool wear, all cutting tests were carried out at a fixed volume of metal removed (300 mm^3). Table 2 summarizes the tool data.

Dry turning tests were carried out on a 10 HP Standard Modern NC lathe. The cutting force components (Fx, Fy, Fz) and tool wear were measured continuously for each combination of cutting parameters. The tool forces were measured using a Kistler 3-component dynamometer and the cutting conditions were selected carefully for each tool material. In some of the cutting tests, the tool temperature was measured using K-type thermocouples that were glued onto the tool rake face, 1 mm away from the cutting edge. The reliability of the measurement techniques was checked constantly by repeating the experiments and the results of each set of experiments were accepted if they exhibited a variance of less than 5%. At the end of each cutting test, the tool wear was examined using a scanning electron microscope and the X-ray dispersion technique. The tool flank wear (VB) was measured using a toolmaker's microscope.

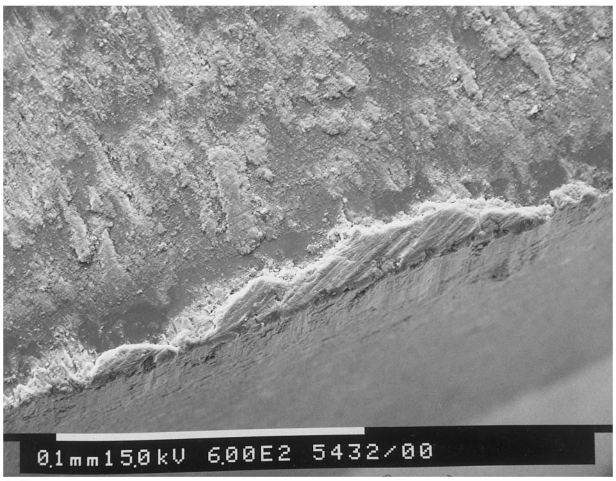

(a)

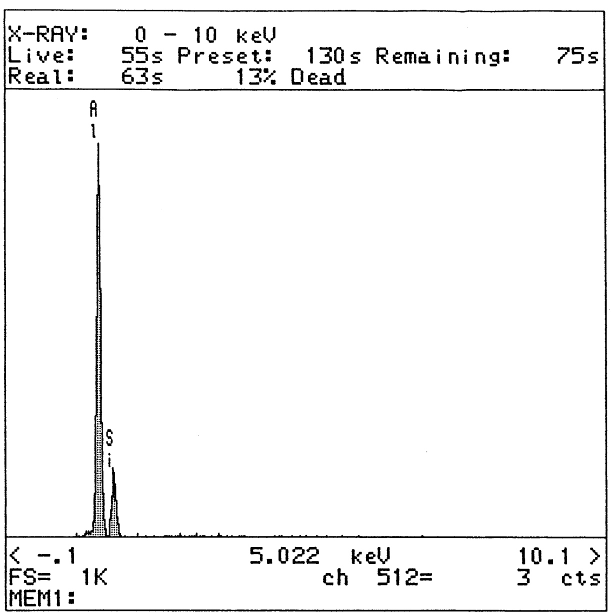

(b)

Fig. 4. (a) Built-up edge on PCD tools ($v = 670$ m min^{-1}, $f = 0.25$ mm rev^{-1}, $doc = 2.5$ mm, $r = 1.6$ mm, $\alpha = 0°$); (b) X-ray dispersion of built-up edge shown in Fig. 4(a).

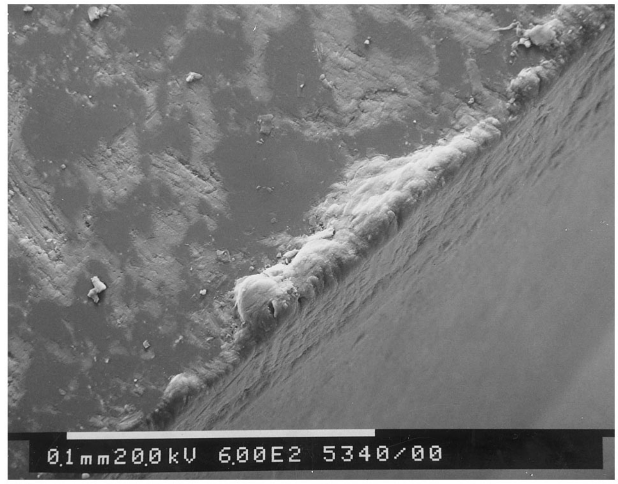

(a)

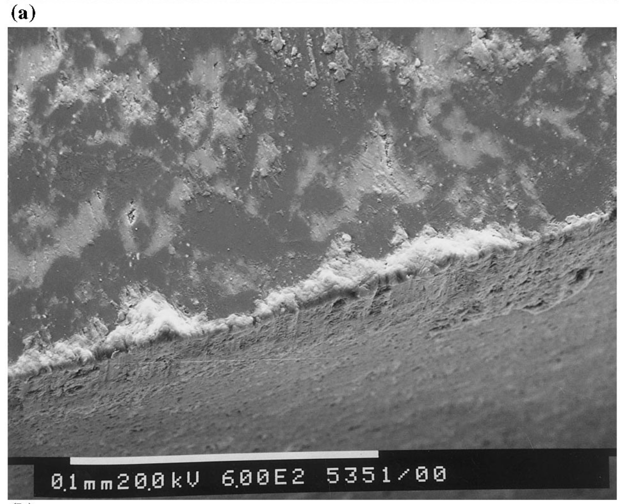

(b)

Fig. 5. (a) Built-up edge on PCD tools ($v = 670$ m min^{-1}, $f = 0.45$ mm rev^{-1}; $doc = 2.5$ mm, $r = 1.6$ mm); (b) as for Fig. 5(a), but for $v = 894$ m min^{-1}.

4. Results and discussion

4.1. Effect of tool material

A series of preliminary tests was conducted to asses the effect of tool material on the tool wear, cutting forces and cutting temperature during the rough turning of 20%SiC/Al PMMC. Fig. 1 shows that Al_2O_3/TiC tools suffered excessive wear in the form of edge chipping. Al_2O_3 particles are pulled out by the abrading workpiece particles, which have a greater Vickers hardness number (VHN) than the Al_2O_3 particles (VHN for Al_2O_3TiC = 2500 kg$_f$ mm^{-2}; VHN for SiC = 3000 kg$_f$ mm^{-2}). Crater wear was also observed, which is due to the widening of grooves that were caused by abrasion. Due to severe edge chipping, the cutting forces for the

Al_2O_3/TiC tool were much higher than those experienced by TiN coated tools (Table 3). The TiN coating provided some protection against the abrasive effects of the SiC particles. The superior performance of polycrystalline diamond tools, compared to both Al_2O_3/TiC and TiN coated carbide tools, is attributed to their high abrasion resistance and high thermal conductivity, which led to lower cutting temperatures, as shown in Table 3. Therefore, all machinability studies carried out thereafter were concerned with the optimization of the cutting process using PCD tools.

4.2. Effect of cutting parameters

Figs. 2 and 3 show that as the cutting speed and/or the depth of cut increase, the cutting forces decrease. This could be attributed to thermal softening of the workpiece material. Another possible reason is due to the changes introduced into the tool geometry upon the formation of built-up edge. Fig. 4(b) shows the X-ray dispersion of the built-up material shown in Fig. 4(a).

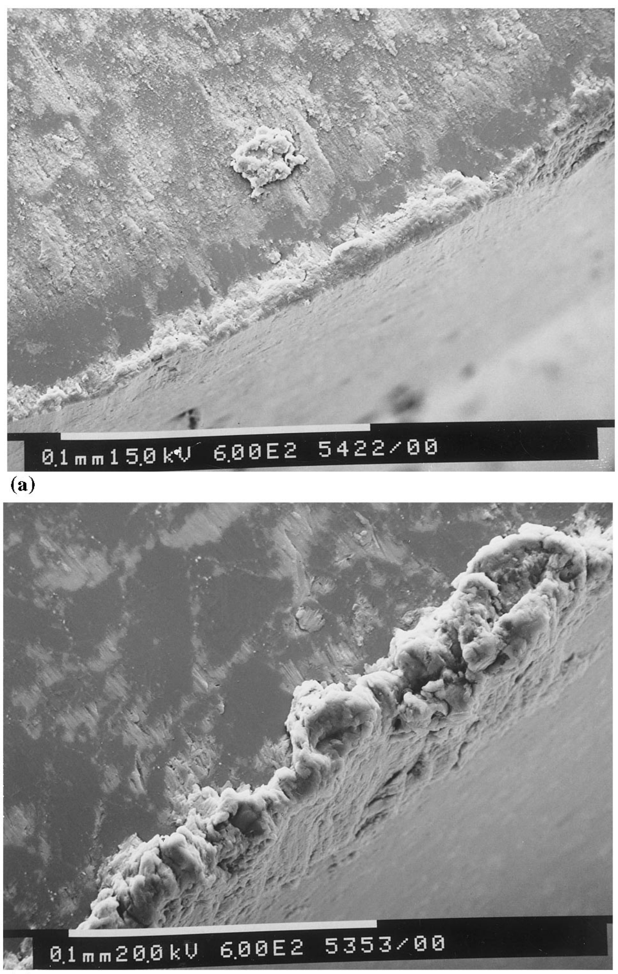

Fig. 6. (a) Built-up edge on PCD tools ($v = 670$ m min^{-1}, $f = 0.35$ mm rev^{-1}, $doc = 1.5$ mm, $r = 1.6$ mm, $\alpha = 0°$); (b) as for Fig. 6(a), but for $doc = 2.5$ mm.

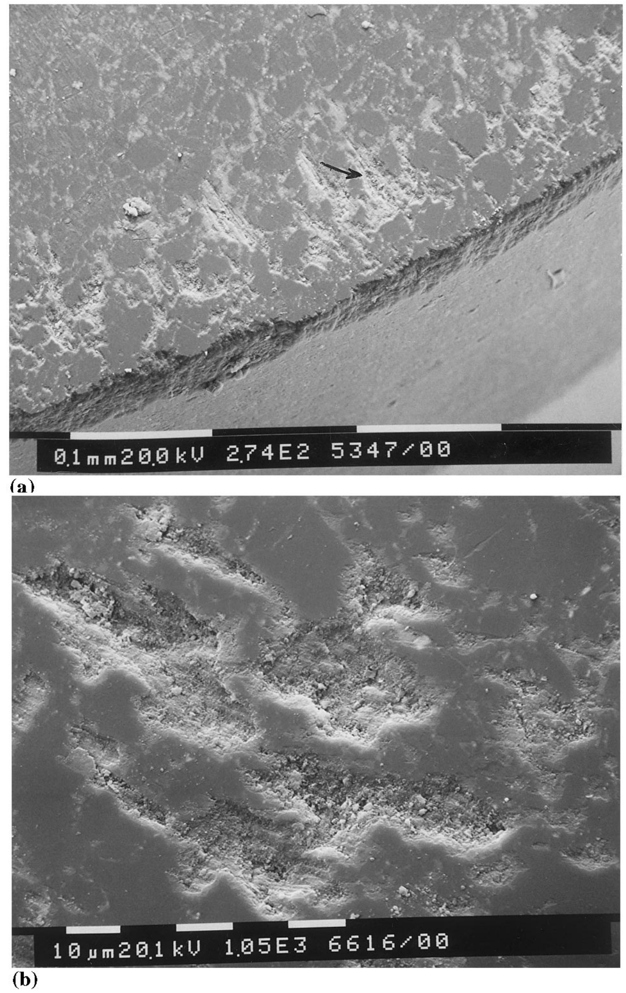

Fig. 7. (a) SEM image illustrating the wear on the PCD tool rake face after dissolving the BUE with NaOH ($v = 670$ m min^{-1}, $f = 0.15$ mm rev^{-1}, $doc = 1.5$ mm, $r = 1.6$ mm, $\alpha = 0°$); (b) higher magnification of rake face of the tool shown in Fig. 7(a).

Built-up edge was observed in all tools under all cutting conditions. This is because particulate SiC/Al MMCs have all of the characteristics of materials that form

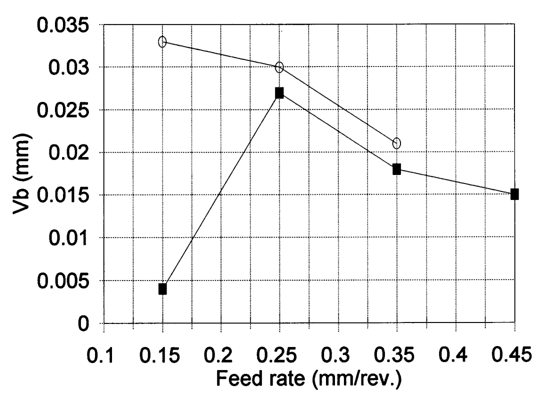

Fig. 8. Effect of cutting speed on the tool flank wear (PCD tool: $r = 1.6$ mm, $\alpha = 0°$; square points: $v = 670$ m min^{-1}, $doc = 1.5$ mm; round points: $v = 894$ m min^{-1}, $doc = 1.5$ mm).

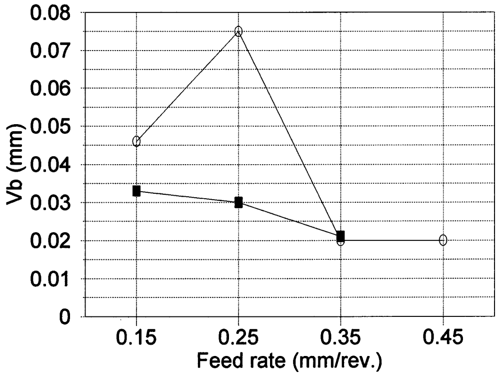

Fig. 9. Effect of depth of cut on the tool flank wear (PCD tool: $r = 1.6$ mm, $\alpha = 0°$, $v = 894$ m min^{-1}; square points: $doc = 1.5$ mm; round points: $doc = 2.5$ mm).

BUE (i.e. strain-hardened two-phase material under high temperature and pressure).

At high cutting speeds ($v = 894$ m min^{-1} (Fig. 5(b)), a smaller BUE is formed, compared to the BUE formed at $v = 670$ m min^{-1} (Fig. 5(a); the height of the BUE was measured perpendicular to the rake face) In contrast, by increasing the depth of cut from 1.5 to 2.4 mm, a large BUE is formed (Fig. 6(a,b), which could break off the tool causing tool chipping and consequent adverse effects on the workpiece surface roughness and dimensional accuracy.

Topographies of the tool indicate that the main wear mechanism of PCD is abrasion (manifested as grooves parallel to the chip flow direction). These grooves could be attributed to three factors. The first is that Al_2O_3 is formed at the tool edge, which is hard enough to produce grooving wear in the PCD. The second explanation for the PCD grooving is aluminium seizure and the pull-out process of the PCD grain, as shown in Fig. 7(a,b). The third possible reason behind PCD grooving is that SiC particles abrade the tools. Thus, PCD tools with PCD grains larger than the grain size of the SiC particles could better withstand the abrasion and 'micro-cutting' by the SiC particles. However, one should note that as the size of the PCD grains increases, the fracture properties of the PCD tool deteriorates, due to an increased number of flaws in the material.

The grooves that were formed on the tool face were filled with the workpiece material. This adhering layer somewhat protected the tool's rake face against further abrasion. Nonetheless, the tool flank face continued to be subjected to abrasion. Hence, flank wear (Vb) was taken as the tool life criterion with $Vb_{1im} = 0.18$ mm. Fig. 8 shows that as the cutting speed increases, the flank wear increases. This could be attributed to the increase in the kinetic energy of the abrading particles, as previously hypothesized by Lane [17].

Increasing the depth of cut leads to an increase in the flank wear (Fig. 9). This is attributed to enhanced abrasion by micro-cutting at the tool flank face. To illustrate this point, in the case of a greater depth of cut a larger surface area of the tool flank face is exposed to abrasion.

Increasing the feed rate had a beneficial effect. As shown in Figs. 8 and 9, as the feed rate increases, the tool wear decreases. In the case of higher feed rates, for a fixed volume of metal removal, the tool surfaces will have less contact with the abrasive PMMC. Another

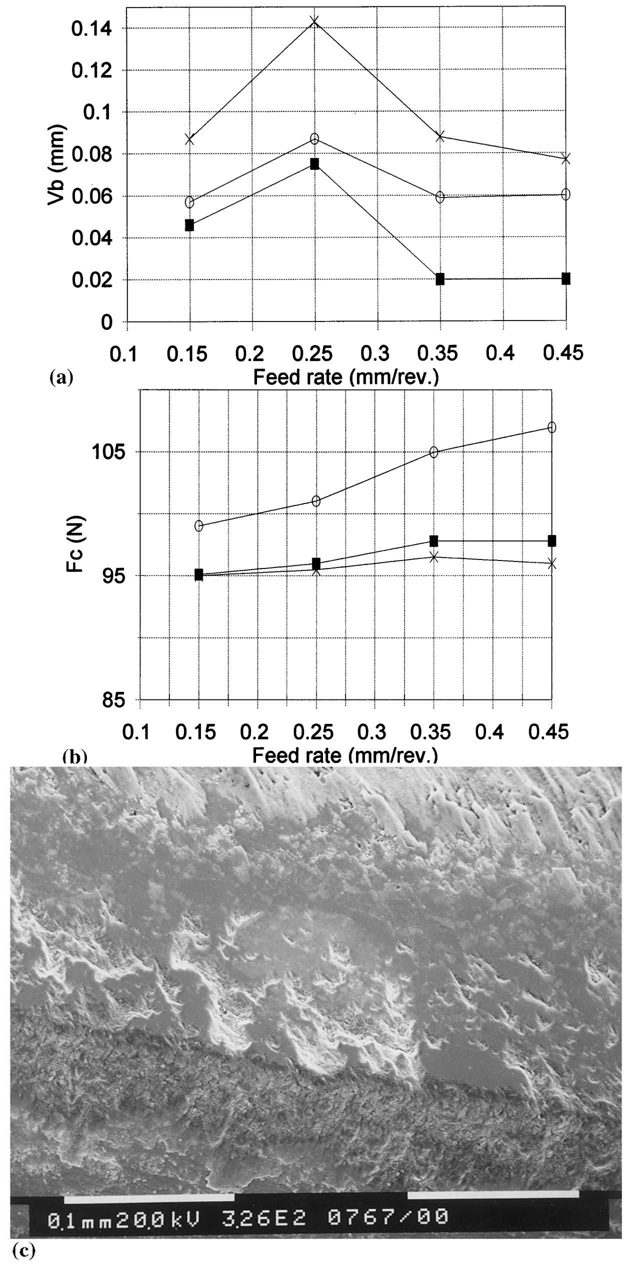

Fig. 10. (a) Effect of PCD tool rake angle on tool flank wear ($v = 894$ m min^{-1}, $doc = 2.5$ mm, $r = 1.6$ mm; square points: 0°; round points: -5; star points, $+5°$); (b) effect of PCD tool rake angle on the cutting forces ($v = 894$ m min^{-1}, $doc = 2.5$ mm, $r = 1.6$ mm; square points: 0°; round points: -5; star points, $+5°$); (c) SEM image illustrating the PCD tool wear by pitting ($v = 670$ m min^{-1}, $doc = 1.5$ mm, $f = 0.25$ mm rev^{-1}, $r = 1.6$ mm, $\alpha = +5°$).

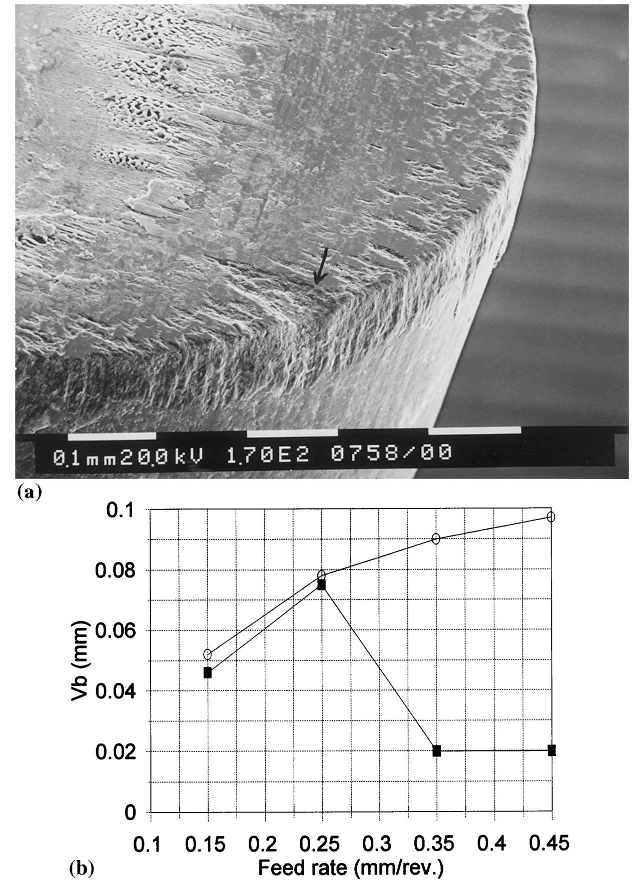

Fig. 11. (a) SEM image illustrating the PCD tool wear by chipping ($v = 894$ m min^{-1}, $doc = 1.5$ mm, $f = 0.35$ mm rev^{-1}, $r = 0.8$ mm, $\alpha = 0°$); (b) effect of tool nose radius on the tool flank wear ($v = 894$ min, $doc = 2.5$ mm, $\alpha = 0°$; tool FW: square points, $r = 1.6$ mm; round pitch points, $r = 0.8$ mm).

advantage gained by increasing the feed rate is the change in chip form. At low feed rates, the chips formed were continuous, also being difficult and hazardous to handle. At high feed rates and high depths of cut ($f > 0.35$, $doc > 2.0$ mm), the chips formed were discontinuous. Despite the fact that in all experiments with PCD tools high feed rates resulted in lower tool wear, a conclusive decision about the optimum cutting parameters should take into consideration the effect of the cutting parameters on the surface integrity and sub-surface damage produced in the workpiece. Comprehensive analysis of the surface integrity and chip morphology will be presented in the Part II of this research study.

4.3. Effect of tool geometry

The tool rake angle had a profound effect on the wear of PCD tools. Three different rake angles were examined. As can be seen from Fig. 10(a), tools with 0° rake angle out-performed positive and negative rake angle tools. A possible reason for the increased flank wear in the case of negative rake angle, is the greater cutting forces encountered with such a rake angle (Fig. 10(b)). Moreover, the chips produced became caught between the tool and the workpiece, causing damage to the tool surface. Tools with positive rake angle showed irregular flank wear and excessive pitting in the cutting edge zone, as shown in Fig. 10(c).

The tool nose radius plays a key role in determining the wear mode of the tool. As the tool nose radius was decreased from 1.6 to 0.8 mm, the tool was found to suffer from excessive chipping and crater wear, as shown in Fig. 11(a). This tool chipping leads to an increase in cutting forces and flank wear, as shown in Fig. 11(b). Tools with small nose radii are thus recommended for finishing operations where light cutting parameters are used. Small nose radii are also expected to yield better geometrical accuracy.

5. Conclusion

The results of the machinability studies carried out on 20%SiC/Al particulate metal-matrix composites indicated the following.

(1) The main tool wear mechanism is abrasion and micro-cutting of tool material grains, manifested as grooves on the tool face parallel to the chip flow direction. All of the tools tested also suffered from flank wear due to abrasion. There was no evidence of chemical wear (e.g. by diffusion).

(2) PCD tools sustained the least tool wear compared to TiN coated carbide tools and Al_2O_3/TiC tools. This is undoubtedly due to PCD's superior hardness and wear resistance, as well as low coefficient of friction, together with high thermal conductivity. This led to lower cutting temperatures when PCD tools were employed. On the other hand, the TiN coated carbide tools and Al_2O_3/TiC tools suffered from excessive crater wear and edge chipping.

(3) The grooves formed on the rake face of PCD tools were filled with smeared workpiece material. This form of built-up edge is beneficial, since it protects the tool rake from further abrasion.

(4) The cutting parameters play a key role in determining the amount of tool flank wear, as well as the size of the built-up edge. Tool wear is minimized by increasing the feed rate, which leads to a reduction in contact between the tool and the abrading SiCp. Although increasing the cutting speed is expected to accelerate the flank abrasion wear dramatically, the results indicated that the increase in wear is minimal. Higher cutting speeds were associated with the increase in the cutting temperatures, which led to the formation of a 'protective' sticking thin layer of workpiece material on the tool. This form of 'protective built-up edge' was prevented from growing in size by the increase speed of

rubbing. Within the tested range of cutting parameters, the speed of 894 m min^{-1}, $f = 0.45$ mm rev^{-1} and depth of cut = 1.5 mm resulted in the smallest tool wear. These cutting parameters enhance the productivity rates upon using PCD tools.

(5) PCD tools with nose radii = 16 mm and rake angle = 0° also led to lower flank wear.

Acknowledgements

The authors would like to thank R. Bruski, from Duralcan, USA and D. Dyer from GE Superabrasives, for supplying the test material and cutting tools and for their helpful comments throughout the research project. The experiments were conducted in the machining laboratories of the Intelligent Machines and Manufacturing Research Center at McMaster University.

References

[1] P. Rohatgi, Advances in cast MMCs, Adv. Mater. Process. 2 (1990) 38–44.
[2] J.M. Monaghan, The use of quick-stop test to study the chip formation of an SiC/Al metal matrix composite and its matrix alloy, Process. Adv. Mater. 4 (1994) 170–179.
[3] B. Boardman, Metal Matrix Composites—An Opportunity for the Off-Highway Industry, SAE International, OH, USA, 1990.
[4] S. Ramrattan, F. Sitkins, M. Nallakatala, Optimization of the casting and machining processes for a metal-matrix composite, Proc. Canadian Soc. Mech. Eng. Symp., McMaster University, 1996, pp. 624–629.
[5] N. Tomac, K. Tonnessen, Machinability of particulate aluminum matrix composites, CIRP Ann. 41 (1992) 55–58.
[6] J. Monaghan, P. O'Reilly, Machinability of aluminum alloy/silicon carbide metal matrix composite, Process. Adv. Mater. 2 (1992) 37–46.
[7] M.K. Brun, M. Lee, Wear characteristics of various hard materials for machining SiC-reinforced aluminum alloy, Wear 104 (1985) 21–29.
[8] K. Winert, A consideration of tool wear mechanism when machining metal matrix composites (MMC), CIRP Ann. 42 (1993) 95–98.
[9] L. Cronjager, Machining of fibre and particle-reinforced aluminum, CIRP Ann. 41 (1992) 63–66.
[10] I.E. Clark, A Guide to machining metal composites with syndite PCD', Mach. Guide, (March 1994) 135–138.
[11] J. Vaccari, C. Lane, Machining a new breed of aluminum, Am. Machinist (November 1993) 56–60.
[12] C. Lane, Drilling and tapping of SiC particle reinforced aluminum, Proc. Machining of Composite Materials Conf., ASM International, Pittsburg, PA (October 1993).
[13] C. Lane, M. Lennox, Economics of machining cast MMC brake rotors, Duralcan Report, 1994, pp. 1–8.
[14] C. Lane, Machining discontinously-reinforced aluminum composites, in: Tool and Manufacturing Engineers Handbook, Vol. 7, Society of Manufacturing Engineers, 1983.
[15] C. Lane, Machinability of aluminum composites as a function of matrix alloy and heat treatment, Proc. Machining of Composite Materials Symp., ASM International, Chicago, IL, (November 1992).
[16] Face milling, end milling, drilling, reaming and tapping of SiC/A356 cast aluminum—Duralcan designation no. F3A.15S-metal matrix composite, Metcut Report No. 2852-495123-3, 1990, pp. 1–7.
[17] C. Lane, The effect of different reinforcements on PCD tool life for aluminum composites, Duralcan Report, 1995, pp. 1–6.
[18] C. Lane, M. Finn, Observations on using CVD diamond in milling MMCs, Proc. Symp. on Materials Issues in Machining and the Physics of the Machining Process', TMS, Chicago, IL, (November 1992).
[19] C. Lane, M. Finn, A comparison of PCD and CVD diamond in milling MMCs, Proc. Symp. on Advances in Production and Fabrication of Light Metals and Metal Matrix Composites, CIM, Edmonton, Alta., Canada (August 1992).
[20] Duralcan composites for gravity castings, Duralcan Report, 1996, pp. 1–4.
[21] Duralcan composites for high-pressure die castings, Duralcan Report, 1996, pp. 1–6.
[22] Duralcan composites-machining guidelines, Duralcan Report, 1995, pp. 1–5.
[23] C. Lane, The state of the art in manufacturing with MMCs, Duralcan Report, 1994, pp. 1–7.
[24] M. Finn, A. Srivastava, Machining of advanced and engineered materials CSME Symp., McMaster University (1996) pp. 616–623.
[25] E. Morin, J. Masoounave, E.E. Laufer, Effect of drill wear on cutting forces in drilling of metal matrix composites, Wear 184 (1995) 11–16.